

## Computationally efficient determination of hydrogen isotope effects on the thermodynamic stability of metal hydrides

Kelly M. Nicholson and David S. Sholl

*School of Chemical & Biomolecular Engineering, Georgia Institute of Technology, 311 Ferst Drive, Atlanta, Georgia 30332-0100, USA*  
(Received 8 August 2012; revised manuscript received 2 October 2012; published 19 October 2012)

Although the thermodynamics of metal hydrides at low to moderate temperatures has been successfully described with density functional theory (DFT) calculations using 0 K total energies and simple harmonic models, it is unclear if this approach is valid for hydrides that are stable at high temperatures. To aid development of computationally efficient methods, this paper uses DFT to explore the predicted stabilities of  $ZrH_2$ ,  $HfH_2$ ,  $TiH_2$ ,  $LiH$ , and  $NaH$  with four levels of theory. We also investigate isotope effects to understand if these should be accounted for in screening of deuterated or tritiated materials. We show that calculations that account for vibrational corrections to the crystal lattice are not necessary to get an accurate description of relative stabilities of metal hydrides. The shifts in dissociation temperatures due to isotope substitutions are  $<50$  K for all materials, with larger shifts for lighter materials, as expected. We show that accounting for vibrational effects due to isotope substitution in metal hydrides is unnecessary to accurately predict the relative stabilities of metal hydrides at high temperatures.

DOI: [10.1103/PhysRevB.86.134113](https://doi.org/10.1103/PhysRevB.86.134113)

PACS number(s): 65.40.-b, 65.40.De, 28.60.+s

### I. INTRODUCTION

In accordance with the Energy Policy Act of 2005, the US Department of Energy (DOE) Next Generation Nuclear Plant (NGNP) project seeks to demonstrate advanced nuclear technologies that provide low-carbon process heat and economical electricity to consumers.<sup>1,2</sup> The DOE has specified the NGNP prototype reactor will be a very-high-temperature gas-cooled reactor with core outlet temperatures in the range of 1000 to 1200 K.<sup>1</sup> The helium coolant from this reactor may be used to provide high-temperature process heat to industrial users, but contamination from tritium, a radioactive fission product, must be removed from the coolant to enable this application.<sup>2</sup> One potential avenue for removing tritium from this gas mixture is to use metals as getters to absorb tritium in the form of metal tritides. Because of the considerable practical difficulties with doing experiments involving tritium at high temperature, computational methods that can reliably predict the performance of candidate getter materials would be useful. Many computational studies based on density functional theory (DFT) have been used to determine mechanical, thermodynamic, and electronic properties of metal hydrides.<sup>3-8</sup> Additionally, DFT-based methods have made useful contributions for crystal-structure prediction,<sup>9-14</sup> material screening for other applications involving formation of metal hydrides,<sup>12,15-23</sup> and development of metal membranes for hydrogen purification.<sup>24-34</sup> In this paper, we consider the challenge of using DFT-based methods to make accurate predictions about isotope effects on the stability of metal hydrides at high temperatures.

Metal hydrides such as Zr-H and LiH, stable to temperatures in excess of 1000 K, have found several uses in nuclear applications as components of nuclear fuels and as neutron moderators since the 1950s.<sup>35-39</sup> Recently, metal hydride systems have been studied extensively as potential hydrogen storage media for hydrogen-powered automobiles due to their high capacity and safety relative to gaseous or liquid storage options. Thus, research efforts have focused predominantly

on identifying metal hydride systems that release appreciable hydrogen at or around room temperature rather than those that operate at conditions relevant for the NGNP reactor.<sup>40,41</sup>

Polyatomic crystals, including metal hydrides, are known to experience isotope effects such as the contraction of the unit cell with substitution of  $^2H$  (D) and  $^3H$  (T) isotopes (deuterides and tritides) relative to  $^1H$  (H)-substituted metal hydrides (protides).<sup>42,43</sup> Thermodynamic models that account for temperature- and/or volume-dependent lattice vibrations can predict structural changes due to isotope substitution. For example, Hu *et al.* quantified the zero-point energy corrections to the lattice constants of  $TiX_2$  ( $X = H, D, T$ ) using a quasiharmonic approach to describe the vibrational properties of the solids.<sup>44</sup> Hu *et al.* and Zhang *et al.* studied the relative thermodynamic stabilities of  $TiH_2$  and  $LiH$  substituted with hydrogen isotopes using density functional perturbation theory (DFPT).<sup>38,44</sup> Directly comparing the temperature-dependent free energies of the protide, deuteride, and tritide species, both authors concluded that the metal tritides are more stable than the corresponding metal hydrides over wide temperature ranges. This conclusion, however, did not account for isotope effects in the gas-phase species ( $H_2$ ,  $D_2$ , or  $T_2$ ). We show in the following that accounting for these effects leads to a revision of these earlier conclusions.

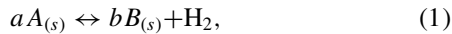
In this paper, we determine the minimum level of theory that will allow for sufficient accuracy in describing the thermodynamic stability of metal hydrides using DFT for material screening purposes. We use the temperature at which a metal hydride is in equilibrium with 1 bar of hydrogen gas,  $T_d$ , to rank materials. Metal hydrides with higher  $T_d$  can operate to higher temperatures in gettering applications. We assess the capabilities of our minimum level of theory in describing the relative stabilities of  $NaH$ ,  $LiH$ ,  $TiH_2$ ,  $ZrH_2$ , and  $HfH_2$ . These systems form particularly stable metal hydrides and exhibit a range of metal-hydrogen bonding characteristics.  $LiH$  and  $NaH$  exhibit strong ionic bonding, whereas the transition-metal hydrides form interstitial structures with metallic-type bonds.<sup>45</sup> This list also spans a wide range in metal atomic

weights, from  $6.941 \text{ g mol}^{-1}$  for Li to  $178.49 \text{ g mol}^{-1}$  for Hf. In addition, we use different levels of theory to clarify the effect of hydrogen isotopes in metal hydrides, particularly the magnitude of the zero-point-energy correction to ground-state unit-cell volumes and relative  $T_d$ , to establish if isotope effects should be accounted for in material screening for the NGNP application.

## II. THEORETICAL METHODS

### A. Free energy

The thermodynamic stability of a metal hydride can be described via the Gibbs free-energy difference between the metal hydride and its decomposition products,  $\Delta G$ . For dehydrating reactions of the type



where  $A$  and  $B$  are the metal hydride and pure metal phases, respectively,

$$\Delta G(T) = bG_B + G_{\text{H}_2} - aG_A, \quad (2)$$

and  $\Delta G < 0$  indicates the reaction in Eq. (1) proceeds to the right. Assuming the activity coefficients for the solid phases are unity, the van 't Hoff relation relates the free-energy difference to the hydrogen pressure at equilibrium:<sup>19,46</sup>

$$\frac{P}{P_0} = \exp\left(\frac{-\Delta G(T)}{RT}\right), \quad (3)$$

where  $P_0 = 1 \text{ bar}$ . We define  $T_d$  as the temperature at which  $P = 1 \text{ bar H}_2$ , or equivalently, where  $\Delta G(T) = 0$ .

The Gibbs free energy is defined as

$$G = U - TS + PV = F + PV, \quad (4)$$

where  $U$ ,  $S$ , and  $F$  are the internal energy, entropy, and Helmholtz free energy, respectively. As noted by Ackland, it is usually computationally simpler to determine  $F$  rather than  $G$  for solids since the Hamiltonian can be constructed as a function of volume rather than of pressure.<sup>47</sup> For the system in Eq. (1), it is assumed that  $\Delta(PV)_{\text{solids}} \ll (PV)_{\text{H}_2}$ .<sup>19</sup>  $F$  will be used in this paper when referring to the free energy of a metal hydride or metal, and  $G$  for the gas phases is determined from a combination of experimental and DFT data as discussed below.

Using the form adopted by Grabowski,  $F$  can be written as a sum of electronic and vibrational contributions.<sup>48,49</sup> The vibrational contribution can be further divided into quasiharmonic and anharmonic correction terms  $F^{\text{qh}}$  and  $F^{\text{anh}}$ , respectively. This gives

$$F(V, T) = E_0(V) + F^{\text{qh}}(V, T) + F^{\text{anh}}(V, T), \quad (5)$$

where  $E_0(V)$  is the ground-state total energy of a crystal determined using DFT. Finite-temperature electronic excitations are neglected in these calculations. In Eq. (5), the quasiharmonic free-energy contribution accounts for volume-dependent zero-point and finite-temperature vibrational effects in solids within the harmonic approximation. For a given volume, the phonon density of states is computed and integrated to give the temperature-dependent vibrational free energy within the harmonic approximation.<sup>47</sup> In this paper, the phonon density of

states is computed using the direct method as implemented by Parlinski and is hereafter referred to as a phonon calculation.<sup>50</sup>  $F^{\text{anh}}$  corrects for the fact that the phonon frequency  $\omega$  is a function of both  $V$  and  $T$ . Wu's method<sup>51</sup> of determining  $F^{\text{anh}}$  using *ab initio* calculations within the framework developed by Wu and Wentzcovitch<sup>52</sup> is utilized to complete the definition of Eq. (5).

### B. Levels of theory to predict $F(V, T)$

Several levels of theory are embedded in  $F(V, T)$  as defined in Eq. (5). Each level makes assumptions regarding which phenomena are relevant, and the higher levels require significantly more computational effort than lower levels. Additionally, there are several methods for calculating terms within a given level of theory. In this paper, we determine the free energies of metal hydrides and corresponding pure metal phases with four levels of theory to assess the relative benefit of the added computational cost for higher levels.

The simplest level of theory based solely on ground-state energy calculations neglects the temperature dependence of the free energy. The free energy approximated in this way may either neglect or include zero-point vibrational energies:

$$F(V_0) \cong E_0(V_0), \quad (6)$$

$$F(V_0) \cong E_0(V_0) + F^{\text{qh}}(V_0, T = 0). \quad (7)$$

Computations at this level simply involve computing the total energy of the solid phases at the uncorrected ground-state equilibrium volume  $V_0$  using DFT.  $V_0$  is uncorrected because it does not include the shift in equilibrium volume due to zero-point vibrational effects.<sup>44</sup> We use phonon calculations to determine zero-point energies in this paper. Since  $\Delta G = \Delta H(T) - T\Delta S(T)$  and  $\Delta G$  behaves largely linearly beyond the low-temperature regime,  $T_d$  can be approximated using

$$T_d = \frac{\Delta H}{\Delta S} \quad (8)$$

with  $\Delta H \approx \Delta F(V_0)$  and  $\Delta S \approx 0.130 \text{ kJ K}^{-1} \text{ mol}^{-1} \text{ H}_2$  as proposed by Zuttel *et al.* for all metal-hydrogen systems.<sup>53</sup>

Ground-state energy calculations have been widely applied to determine properties of metal hydrides at low to moderate temperatures. For example, Ackland used DFT to identify the bistable crystal structure of  $\epsilon\text{-ZrH}_2$  using ground-state energy calculations.<sup>10</sup> Alapati *et al.* screened over 300 metal hydride systems for use in reversible  $\text{H}_2$  storage applications based on reaction enthalpies calculated via the relation  $\Delta H(T) \approx \Delta E_0$  plus a correction term.<sup>19</sup> They found that the zero-point energies were partially offset by the  $\text{H}_2$  translational, rotational, and  $PV$  contributions to the free energy and that these terms could be approximated with an empirical correction term.

Simple harmonic models introduce finite-temperature vibrational effects in solid phases through a single phonon calculation at either the uncorrected or corrected ground-state volume. The key difference between this and higher levels of theory is that the phonon frequency dependence on volume and temperature and, thus, thermal expansion, are neglected.

The free energy of each solid in this approach is approximated by

$$F(V_0, T) \cong E_0(V_0) + F^{\text{qh}}(V_0, T), \quad (9)$$

$$F(V_{0c}, T) \cong E_0(V_{0c}) + F^{\text{qh}}(V_{0c}, T), \quad (10)$$

where the first (second) expression uses the uncorrected (corrected) ground-state volume. Zhu *et al.* used this approach to study  $\gamma$ -ZrH,  $\zeta$ -Zr<sub>2</sub>H,  $\varepsilon$ -ZrH<sub>2</sub>, and  $\delta$ -ZrH<sub>1.5</sub>.<sup>37</sup>

The third level of theory we consider is a quasiharmonic model in which the dependence of phonon frequencies on volume is included:

$$F(V, T) \cong E_0(V) + F^{\text{qh}}(V, T). \quad (11)$$

Quasiharmonic models involve significantly more computational effort than lower levels of theory because  $\omega = \omega(V)$  must be calculated for a range of volumes rather than at a single volume. Since the free-energy surface has both volume and temperature degrees of freedom, the equilibrium volume is that which minimizes  $F(V)$  at a given temperature. Thus, this calculation predicts how the volume of the solid expands or contracts with temperature. The relative computational cost for computing the free energy for a solid within a simple harmonic or quasiharmonic model depends greatly on the symmetry of the crystal structure and the number of volumes sampled to describe the volume-dependent free energy.

There are two common approaches to sampling the volume in the quasiharmonic approximation. The full-search method varies each lattice degree of freedom independently while simultaneously relaxing ionic positions and determines  $\omega$  and  $F(T)$  for each unique configuration. This method can be very computationally expensive for materials with multiple degrees of freedom, but has successfully been applied to simple materials such as hcp Mg, Ti, and Zr to study anisotropic thermal expansion.<sup>54</sup> The volume-only stress-minimization method, referred to as the static quasiharmonic method in this paper, is less demanding in that phonon frequencies are only computed at specific volumes in a selected range of volumes where the lattice parameters and atomic coordinates are those that minimize the electronic total energy  $E_0(V)$ . Carrier *et al.* found good agreement between predicted lattice constants and internal ion positions of MgSiO<sub>3</sub> from static quasiharmonic calculations and experimental results at high  $T$  and  $P$ .<sup>55</sup> Frankcombe and Kroes used both methods to compute the thermal expansion of orthorhombic LiBH<sub>4</sub> with three lattice degrees of freedom. They found that the full-search method led to a 5% greater relaxation in the free-energy minimum compared with the static method, although the quasiharmonic method, in general, did not lead to better agreement with experimental results compared with DFT models neglecting lattice vibrations.<sup>7</sup>

The highest level of theory we consider in this paper includes explicit anharmonic corrections to the quasiharmonic free energy to specify the terms in Eq. (5) in full. Methods for accounting for anharmonic effects in materials due to temperature-dependent phonon-phonon interactions using first principles are still in their infancy and can be computationally expensive.<sup>7,49,56–58</sup> In this paper, calculations at this level required over an order of magnitude more computational effort than models based on the ground-state energy alone, and

this relative effort would be larger for materials with more complex crystal structures. Wu and Wentzcovitch recently developed a semiempirical method to compute the anharmonic contribution based on integration of a parametrized  $F^{\text{anh}}$  with a single constant that can be determined through comparison of predicted and experimental data of a volume-dependent thermodynamic property such as the thermal expansivity.<sup>52</sup> Wu later proposed a method for determining this constant from a single canonical ensemble (NVT) *ab initio* molecular dynamics (AIMD) calculation in combination with the quasiharmonic free energy.<sup>51</sup> Due to its relative computational simplicity, Wu's approach is used in this paper to determine the magnitude of  $F^{\text{anh}}$  for the metal hydrides we consider.

In this paper,  $F(V, T)$  in Eq. (11) was determined using static quasiharmonic calculations for Li, LiX, Na, NaX, Zr, ZrX<sub>2</sub>, Hf, HfX<sub>2</sub>, Ti, and TiX<sub>2</sub> with  $X = \text{H, D, T}$ . For comparison, a quasiharmonic calculation employing the full-search method was completed for hcp Zr and bct ZrH<sub>2</sub> since both crystal structures have two lattice degrees of freedom. In most cases, levels of theory based on ground-state energies and simple harmonic models with or without zero-point lattice corrections [Eqs. (6)–(10)] were determined from Eq. (11) and required no separate computation. Since calculation of the explicit anharmonic correction to the quasiharmonic free energy is computationally expensive, this level of theory was only applied to Zr, ZrH<sub>2</sub>, and ZrT<sub>2</sub>.

### III. COMPUTATIONAL DETAILS

Plane-wave DFT calculations were carried out with the Vienna *ab initio* simulation package (VASP).<sup>59–63</sup> Electronic ground states were determined using the projector augmented wave (PAW) method with the PW91 generalized gradient approximation (GGA) exchange-correlation functional.<sup>64–66</sup> Except where indicated, all calculations were performed on a  $1 \times 1 \times 1$  crystallographic unit cell with a 425 eV cutoff energy and  $9 \times 9 \times 9$   $k$ -point Monkhorst-Pack mesh.  $2 \times 2 \times 2$  supercells were used to compute phonon frequencies, and this was found to be sufficient to reduce the force constant at the supercell surface to three orders of magnitude less than the force constants at the center. All hcp structures were transformed into a rhombohedral setting for calculation of vibrational frequencies. Monkhorst-Pack meshes were adjusted to maintain the same density of  $k$  points for the phonon calculations as used in the electronic total-energy calculations.

Initial crystal structures for metals and metal hydrides were obtained from the Inorganic Crystal Structure Database.<sup>67,68</sup> The elemental metals were treated as hcp Zr, Ti, Hf, and Li and bcc Na based on the structures each adopts at 0 K. The crystal structures of the stoichiometric metal hydrides studied include bct ZrH<sub>2</sub> and HfH<sub>2</sub> and fcc TiH<sub>2</sub>, LiH, and NaH. For agreement with common literature values, the bct lattice parameters are reported in terms of the fct unit cell with the  $a(\text{bct})$  lattice parameter multiplied by a factor of  $\sqrt{2}$ . The temperature-dependent free energy for each volume in a range of volumes was determined to find  $F(V, T)$  for each solid phase. Between 6 and 17 volumes were sampled with the largest set of volumes used to describe light materials. At each volume, the cell shape and ionic coordinates were relaxed until forces on each atom were less than  $10^{-4}$  eV  $\text{\AA}^{-1}$ . The PHONON

code developed by Parlinski was used to calculate the phonon density of states and the vibrational contribution to the free energy using the direct method.<sup>50</sup> A displacement magnitude of  $\pm 0.03$  Å was applied. At each  $T$  examined, a fourth-order polynomial was fit to  $F(V)$ . The error associated with this curve fitting was less than  $0.5$  kJ mol<sup>-1</sup> for HfH<sub>2</sub> and less than  $0.1$  kJ mol<sup>-1</sup> for all other materials.

Since Na and Li melt at 371 and 450 K, respectively, predicting equilibrium volumes at high temperatures for these materials using the quasiharmonic approximation is a mathematical exercise.<sup>69–71</sup> NaH and LiH were predicted to expand beyond the range of volumes sampled for  $T > 630$  K. Since  $\Delta G$  behaves largely linearly beyond the low-temperature regime,  $T_d$  for the quasiharmonic model was determined via a linear fit of  $\Delta G$  between 300 and 630 K for these systems.

For comparison with the static quasiharmonic method, a full-search method was used for anisotropic Zr and ZrH<sub>2</sub>, varying both  $a$  and  $c$  lattice parameters independently and calculating the vibrational free energy at each unique configuration. In the case of hcp Zr, 26 combinations of  $a$  and  $c$  lattice constants with  $\Delta a = 0.01$  Å and  $\Delta c = 0.07$  Å were separately tested for  $a = 3.2 - 3.25$  Å and  $c = 5.1 - 5.45$  Å. Since the vibrational free energy behaves largely linearly with independent changes in  $a$  and  $c$ , the vibrational free energies were slightly extrapolated to extend the range of volumes to  $a = 3.27$  Å. Including volumes beyond these bounds changes the predicted lattice constants by less than  $0.001$  Å. In the case of ZrH<sub>2</sub>, a grid of 63  $a$  and  $c$  combinations with  $\Delta a = 0.03$  Å and  $\Delta c = 0.05$  Å was used for  $a = 3.45 - 3.63$  Å and  $c = 4.35 - 4.75$  Å. A fourth-order polynomial surface was fit to  $F(a, c)$  at each temperature. The lattice coordinates corresponding to the minimum of  $F(a, c)$  were determined using MATLAB's constrained nonlinear optimization functions implemented by a sequential quadratic programming method. The estimated error for this surface fitting was less than  $0.1$  kJ mol<sup>-1</sup>.

Wu's method for determining  $F^{\text{anh}}(V, T)$  in Eq. (5) from a single AIMD calculation is described in Ref. 51. A single AIMD calculation with reciprocal space sampled at the  $\Gamma$  point with a cutoff energy of 425 eV was performed for Zr, ZrH<sub>2</sub>, and ZrT<sub>2</sub>. A  $2 \times 2 \times 2$  48-atom supercell with a volume of  $65$  Å<sup>3</sup> unit cell<sup>-1</sup> for ZrX<sub>2</sub> and a 24-atom supercell with volume of  $58$  Å<sup>3</sup> unit cell<sup>-1</sup> for Zr were tested. Temperature was maintained at 800 K using a Nosé thermostat and Nosé mass corresponding to a period of 40 time steps. The AIMD simulations were run for 6.3 ps including a 2 ps equilibration period with time step of 0.2 fs. The volume-independent dimensionless constants in Wu and Wentzcovitch's model were determined to be  $-0.25$ ,  $-0.36$ , and  $5.25$  for ZrH<sub>2</sub>, ZrT<sub>2</sub>, and Zr, respectively.

Diatomic hydrogen isotope free energies were calculated using

$$G(T) = [G(T) - H_{298.15}] + H_{\text{DFT}, 298.15}, \quad (12)$$

where  $[G(T) - H_{298.15}]$  values were referenced from the Thermodynamics Research Center thermodynamic tables for nonhydrocarbons.<sup>72</sup> These data tables were chosen specifically because they contain references for tritium, for which data are scarce, and they are in agreement with the JANAF tables for H<sub>2</sub> and D<sub>2</sub> within  $2$  kJ mol<sup>-1</sup> over the temperature range studied.<sup>73</sup>

$H_{\text{DFT}, 298.15}$  was calculated for each hydrogen isotope using

$$H(T) = E_0 + U_{\text{vib}}(T) + U_{\text{trans+rot}}(T) + PV. \quad (13)$$

The DFT total energy of a hydrogen molecule was found using a cubic supercell of length  $10$  Å, cutoff energy of 660 eV, and  $2 \times 2 \times 2$   $k$ -point Monkhorst-Pack mesh. These parameters were sufficient to converge  $E_0$  to within  $0.1$  kJ mol<sup>-1</sup>. Finite differences with  $0.01$  Å displacements were used to compute the Hessian matrix and vibrational frequencies at the  $\Gamma$  point of the isotope species in the same cubic supercell. This produced zero-point energies of 26.1, 18.5, and 15.1 kJ mol<sup>-1</sup> X<sub>2</sub> for  $X = \text{H, D, and T}$ , respectively. At 298.15 K, the zero-point energy dominates  $U_{\text{vib}}(T)$  with temperature-dependent contributions of less than  $10^{-3}$  kJ mol<sup>-1</sup>. We assume hydrogen behaves as an ideal gas with  $U_{\text{trans+rot}} + PV = 7/2 RT$ .

#### IV. RESULTS

While the quasiharmonic and explicit anharmonic corrections to the quasiharmonic free-energy levels of theory provide estimates of thermal expansion in solid phases that are unavailable through ground state or simple harmonic free energies alone, it is unclear as to how much incorporating this dependency changes  $T_d$ . To assess these effects, we compare predictions of  $T_d$  for ZrH<sub>2</sub> using four levels of theory. First, we determine the appropriate method for computing free energies within the quasiharmonic approximation for anisotropic Zr and ZrH<sub>2</sub>.

##### A. Full-search versus static quasiharmonic calculation

The unit cells of Zr and ZrH<sub>2</sub> each have two degrees of freedom,  $a$  and  $c$ . Formally,  $F(a, c, T)$ , but the full-search method, which varies each lattice parameter independently and computes the vibrational free energy for each configuration, requires much more computational effort than a static quasiharmonic calculation. Presumably, predictions of  $a(T)$ ,  $c(T)$ , and  $F(T)$  within the quasiharmonic approximation using the full-search method are more accurate than those predicted via the static method. However, the full calculation required six times as many phonon calculations as the static treatment of the free energy based on the lattice grid sampling used in this work. Table I presents the lattice properties of Zr and ZrH<sub>2</sub> determined using both quasiharmonic methods along with comparisons to published experimental and first-principles results. For both Zr and ZrH<sub>2</sub>, the full and static methods produce nearly identical ground-state values for  $a$ ,  $c$ ,  $V$ , and the bulk modulus  $B$  where<sup>44</sup>

$$B = V \frac{\partial^2 F(V)}{\partial V^2}. \quad (14)$$

The DFT results are within 2% of the experimental values for both Zr and ZrH<sub>2</sub>, but accounting for thermal expansion does not bring the predicted values into better agreement with experimental values at 298 K.

Figure 1 shows the predicted lattice expansion and isotropic volume thermal expansion  $\varepsilon$ :

$$\varepsilon = \frac{V - V_{\text{ref}}}{3V_{\text{ref}}} \quad (15)$$



TABLE I. Lattice properties of hcp Zr and fct ZrH<sub>2</sub> at 0 K (298 K) predicted within the quasiharmonic approximation using both full-search and volume-only (static) stress-minimization methods.

	Zr				ZrH <sub>2</sub>			
	<i>a</i> (Å)	<i>c</i> (Å)	<i>V</i> (Å <sup>3</sup> )	<i>B</i> (GPa)	<i>a</i> (Å)	<i>c</i> (Å)	<i>V</i> (Å <sup>3</sup> )	<i>B</i> (GPa)
Full-search	3.230 (3.235)	5.175 (5.180)	46.7 (46.9)	97.6 (94.7)	5.060 (5.058)	4.458 (4.475)	114.1 (114.5)	125.2 (122.1)
Static	3.231 (3.235)	5.174 (5.180)	46.8 (47.0)	97.8 (94.5)	5.045 (5.049)	4.479 (4.486)	114.0 (114.4)	126.4 (123.6)
Experiment	3.227 <sup>a</sup>	5.137 <sup>a</sup>	46.3 <sup>a</sup>	97.2 <sup>b</sup> 95.2 <sup>c</sup>	4.976 <sup>d</sup>	4.451 <sup>d</sup>	110.0	

<sup>a</sup>At 298 K (Ref. 74).

<sup>b,c</sup>At 4 and 298 K, respectively (Ref. 75).

<sup>d</sup>At 297 K (Refs. 76 and 77).

for Zr and ZrH<sub>2</sub> using the full-search and static quasiharmonic methods where  $V_{\text{ref}}$  is the volume at a reference temperature. This definition is consistent with Refs. 54 and 78. For both Zr and ZrH<sub>2</sub>, static calculations predict similar rates of expansion in  $a$  and  $c$ , while in using the full-search method,  $a$  is largely held constant with increasing temperature and expansion in  $c$  drives the overall unit-cell volume expansion. Skinner and Johnston calculate  $\varepsilon = 0.0051$  at 950 K with  $V_{\text{ref}} = V_{298}$  based

on x-ray diffraction measurements of Zr lattice parameters.<sup>74</sup> In comparison, our calculations give  $\varepsilon = 0.0039$  and  $0.0045$  for the full and static methods, respectively, which indicate reasonable agreement with the experimental result. Skinner and Johnston also determine the average linear coefficient of expansion between 298 and 1143 K as  $5.5 \times 10^{-6} \text{ K}^{-1}$  and  $10.8 \times 10^{-6} \text{ K}^{-1}$  for  $a$  and  $c$ , respectively. Our full-search method gives  $3.0 \times 10^{-6} \text{ K}^{-1}$  and  $12.0 \times 10^{-6} \text{ K}^{-1}$  for  $a$  and  $c$ , respectively, for the same temperature range. The static calculation predicts  $7.7 \times 10^{-6} \text{ K}^{-1}$  and  $5.6 \times 10^{-6} \text{ K}^{-1}$  for  $a$  and  $c$ , respectively. Based on this result, the full-search method more accurately predicts the anisotropic thermal expansion of Zr. Over the temperature range studied, the lattice parameters for Zr expand only 0.01 Å in  $a$  and 0.11 Å in  $c$ , which are on the same order as the grid spacing we used to sample lattice configurations for the full method. A more detailed study of the anisotropic thermal expansion of Zr would need to use finer grid spacing. Nie and Xie similarly used DFT to study the thermal expansion of hcp Zr using a full-search quasiharmonic method.<sup>54</sup> While our predicted  $\varepsilon$  with  $V_{\text{ref}} = V_{293}$  are in good quantitative agreement, the predicted lattice parameter expansions agree only qualitatively. Our calculations predict slightly less expansion in  $a$  and more expansion in  $c$  than Nie and Xie. However, this may be due to differences in grid spacing.

The full-search and static quasiharmonic calculations predict virtually identical volumetric thermal expansion for ZrH<sub>2</sub>. Yakel studied the thermal expansion of ZrH<sub>1.92</sub> using x-ray diffraction and found that the linear coefficient of volumetric expansion based on the fct unit cell was  $9.03 \times 10^{-6} \text{ K}^{-1}$  between 300 and 700 K.<sup>42</sup> Our calculations are in excellent agreement with an average linear coefficient of volumetric expansion over the same temperature range of  $10.0 \times 10^{-6} \text{ K}^{-1}$  and  $9.6 \times 10^{-6} \text{ K}^{-1}$  for the full and static methods, respectively. In Yakel's work,  $a$  contracts slightly by about 0.01 Å and  $c$  expands by approximately 0.1 Å between 100 and 800 K. The grid spacing in this work,  $\Delta a = 0.03 \text{ Å}$  and  $\Delta c = 0.05 \text{ Å}$ , is too coarse to perform detailed comparisons of the anisotropic expansion for ZrH<sub>2</sub>. Our calculations indicate, however, that  $a$  tends to expand more slowly than  $c$ , and that the volume expansion is driven by changes in  $c$ .

The predicted free energies for both quasiharmonic methods agree to within 0.3 kJ mol<sup>-1</sup> for ZrH<sub>2</sub> and to within

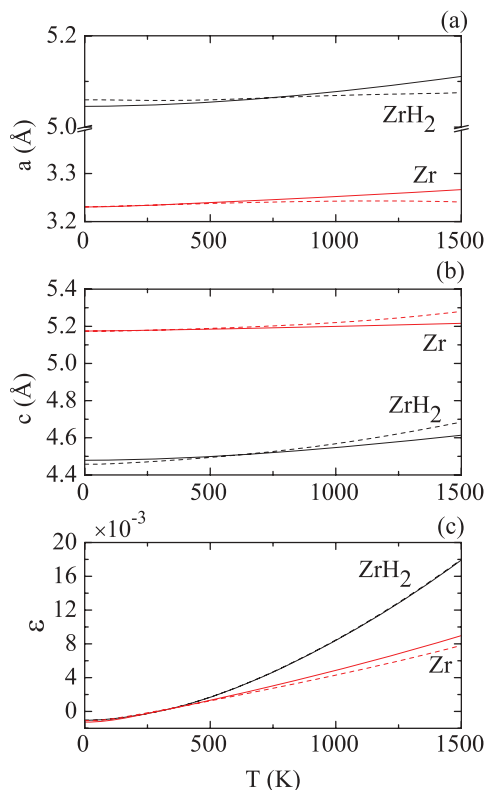


FIG. 1. (Color online) Predicted lattice constants and volume thermal expansion of hcp Zr and fct ZrH<sub>2</sub> within the quasiharmonic approximation using the volume-only (static) stress-minimization (solid curves) and full-search (dashed curves) methods: (a) lattice constant parallel to principal axis, (b) lattice constant perpendicular to principal axis, (c) volumetric thermal expansivity relative to lattice volume at 293 K.

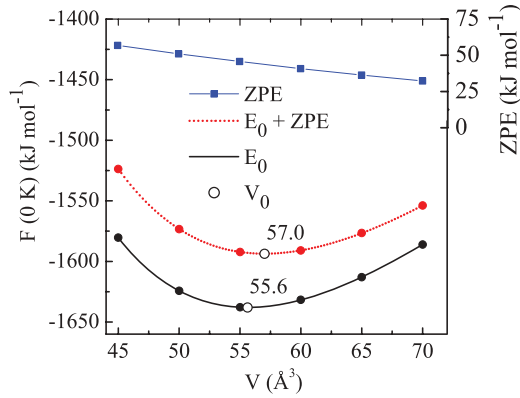


FIG. 2. (Color online) The shift in the  $\text{ZrH}_2$  equilibrium unit-cell volume ( $V_0$ ) at 0 K upon addition of the volume-dependent zero-point-energy (ZPE) correction to the DFT electronic energy ( $E_0$ ).

$0.1 \text{ kJ mol}^{-1}$  for Zr over the full temperature range studied. This corresponds to  $T_d = 1131$  and  $1129 \text{ K}$  for the full-search and static methods, respectively. Thus, static calculations were used in the remainder of this work to calculate  $F(V, T)$  for solid phases within the quasiharmonic approximation.

### B. Simple harmonic free energies

As mentioned above, the computational effort associated with calculating  $\Delta G$  with a simple harmonic calculation at  $V_0$  in Eq. (9) is considerably less than using static quasiharmonic calculations [Eq. (11)]. However, simple harmonic calculations at  $V_{0c}$  in Eq. (10) raise the computational cost to the quasiharmonic level since both methods require computing volume-dependent vibrational energies. Figure 2 shows the slight correction in predicted ground-state volume from  $55.6$  to  $57.0 \text{ \AA}^3$  for  $\text{ZrH}_2$  upon inclusion of zero-point energies. The zero-point-energy lattice correction is even smaller for Zr, with a marginal expansion from  $46.7$  to  $46.8 \text{ \AA}^3$ .

The small corrections to the ground-state volumes of Zr and  $\text{ZrH}_2$  lead to a  $0.7 \text{ kJ mol}^{-1} \text{ H}_2$  difference in  $\Delta H$  at 0 K including zero-point energies and a difference in  $T_d$  of  $15 \text{ K}$ . The difference between these results is likely to be insignificant in terms of material screening. In terms of computational effort, it is, therefore, not cost effective to calculate the volume-dependent zero-point energy to compute  $F(T)$  about the zero-point-energy corrected ground-state volume.

### C. Explicit anharmonic correction

At the temperatures of interest, greater than  $1000 \text{ K}$ , metals and metal hydrides may undergo significant thermal expansion due to temperature-dependent changes in vibrational properties. Often, in first-principles thermodynamic studies of solids, anharmonic contributions are neglected such that  $\omega \neq \omega(T)$  as in the quasiharmonic approximation. While calculations of  $F(V, T)$  within the quasiharmonic approximation [Eq. (11)] include an estimate of anharmonic effects through the temperature dependence of the equilibrium volume, it was unclear how large an error is introduced through not accounting for the explicit anharmonic correction as in Eq. (5). Figure 3 displays the computed anharmonic correction terms for Zr and  $\text{ZrH}_2$ . Incorporation of  $F^{\text{anh}}$  tends to decrease the total free energy of

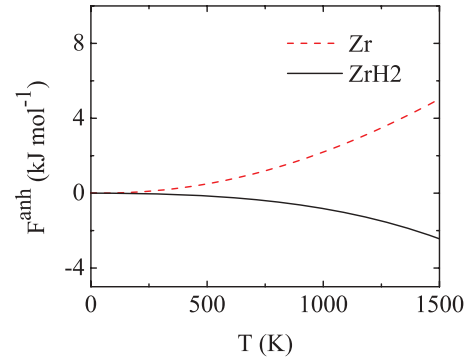


FIG. 3. (Color online) Contribution of the explicit anharmonic free-energy term to the quasiharmonic free energies of Zr and  $\text{ZrH}_2$  determined using the methods of Wu and Wentzcovitch (Refs. 51 and 52).

$\text{ZrH}_2$  and increase the free energy of Zr. However, adjustments are less than  $1 \text{ kJ mol}^{-1} \text{ H}_2$  between 0 and  $500 \text{ K}$ , rising to about  $5.0 \text{ kJ mol}^{-1} \text{ H}_2$  and  $-2.4 \text{ kJ mol}^{-1} \text{ H}_2$  for Zr and  $\text{ZrH}_2$ , respectively, at  $1500 \text{ K}$ . Calculating  $\Delta G$  via Eq. (5) leads to a predicted  $T_d$  of  $1159 \text{ K}$  compared with  $1129 \text{ K}$  computed with quasiharmonic free energies alone. At this temperature,  $\Delta F^{\text{anh}}$  contributes approximately only  $4.5 \text{ kJ mol}^{-1} \text{ H}_2$  to  $\Delta G$ . For  $\text{ZrT}_2$ , the magnitude of  $\Delta F^{\text{anh}}$  at  $T_d$  is nearly the same as for the protiated material, and  $T_d$  similarly increases by  $34 \text{ K}$  relative to the  $T_d$  determined using only static quasiharmonic free energies.

### D. Level of theory comparison

Table II compiles the predicted  $T_d$  of  $\text{ZrH}_2$  for each of the four levels of theory studied in this work. For models based on ground-state energies and simple harmonic calculations, two methods for each level of theory are presented. Of the models that include finite-temperature vibrational effects, i.e., simple harmonic and higher, the difference between the lowest and highest level of theory is only about  $50 \text{ K}$ , which corresponds to an energy difference of about  $7 \text{ kJ mol}^{-1} \text{ H}_2$  based on  $\Delta S \approx 0.130 \text{ kJ K}^{-1} \text{ mol}^{-1} \text{ H}_2$ . Alapati *et al.* calculated the enthalpy of formation for several metal hydride systems including  $\text{MgH}_2$ , LiH,  $\text{CaH}_2$ ,  $\text{AlH}_3$ ,  $\text{Ca}(\text{AlH}_4)_2$ , and  $\text{LiBH}_4$  using both ultrasoft pseudopotentials and PAW methods with the PW91 functional (in Supplemental Material of Ref. 20). Based on these systems, the differences in calculated enthalpy of formation for these two methods ranged from 0 to  $5 \text{ kJ mol}^{-1} \text{ H}_2$ . Similar calculations using the PAW method with PW91 and Perdew-Burke-Ernzerhof (PBE) functionals resulted in differences of  $12 \text{ kJ mol}^{-1} \text{ H}_2$  for LiH and  $10 \text{ kJ mol}^{-1} \text{ H}_2$  for  $\text{MgH}_2$ . Even larger differences were encountered when comparing USPP-PW91 and USPP-rPBE functionals. These results indicate that the predicted thermodynamic properties are more sensitive to the DFT functional than the level of theory used to include finite-temperature vibrational effects.

The finite-temperature models that include thermal expansion of the solid phases (quasiharmonic and the explicit anharmonic correction to the quasiharmonic free energies) exhibit only minor corrections to the simple harmonic models. In the case of the Zr-H system, the magnitude of the static quasiharmonic correction to the simple harmonic

TABLE II. Predicted temperature of dehydrogenation and reaction enthalpy at 0 K for ZrH<sub>2</sub> predicted using four levels of theory ( $V_0$  and  $V_{0c}$  refer to ground-state volumes not corrected and corrected for zero-point vibrational effects, respectively).

Model description	$T_d$ (K)	$\Delta H_0$ (kJ mol <sup>-1</sup> H <sub>2</sub> )
Ground-state energies at $V_0$ [Eq. (6)]	1284	166.9
Ground-state energies including zero-point energies at $V_0$ [Eq. (7)]	1154	150.0
Simple harmonic calculation at $V_0$ [Eq. (9)]	1108	150.0
Simple harmonic calculation at $V_{0c}$ [Eq. (10)]	1123	150.7
Quasiharmonic (static) [Eq. (11)]	1129	150.7
Explicit anharmonic correction to quasiharmonic (static) free energy [Eq. (5)]	1159	150.7

$F(V_0, 1000 \text{ K})$  for ZrH<sub>2</sub> and Zr is only 3 kJ mol<sup>-1</sup> H<sub>2</sub> and 0.2 kJ mol<sup>-1</sup> H<sub>2</sub>, respectively. Thus, the thermal expansion correction is negligible for this system. There is very little difference between the models that account for vibrational contributions to the free energy because  $\Delta G$  largely behaves as a linear function of a constant  $\Delta H$  and  $\Delta S$  beyond the very-low-temperature regime. The models based on ground-state energies rely on the choice of a constant  $\Delta S$ . The good agreement between  $T_d = 1154 \text{ K}$ , predicted for ground-state energies including zero-point energies, and the highest level of theory including anharmonic corrections  $T_d = 1159 \text{ K}$ , is due to the fortuitous use of  $\Delta S \approx 0.130 \text{ kJ K}^{-1} \text{ mol}^{-1} \text{ H}_2$  recommended by Zuttel for all metal-hydrogen systems. The assumed value happens to be very close to that predicted for the anharmonic model with  $\Delta S \approx 0.133 \text{ kJ K}^{-1} \text{ mol}^{-1} \text{ H}_2$  based on linear regression of  $\Delta G$  between 500 and 1500 K. However,  $\Delta S$  has been shown to be as low as  $0.097 \text{ kJ K}^{-1} \text{ mol}^{-1} \text{ H}_2$  for complex metal hydrides such as LiBH<sub>4</sub>.<sup>20</sup> Thus, use of the assumed  $\Delta S \approx 0.130 \text{ kJ K}^{-1} \text{ mol}^{-1} \text{ H}_2$  in ground-state models may not yield results in as good agreement with higher levels of theory in cases where the entropy of reaction is significantly different than the assumed value.<sup>78</sup>

Alapati *et al.* found that  $-20 < \Delta E_{\text{ZPE}}^* + E_{\text{ZPE,H}_2} < -10 \text{ kJ mol}^{-1} \text{ H}_2$  for over 300 metal hydride decomposition reactions including reactions in which the metal hydride is destabilized by another compound where the “asterisk” indicates the change over the solid phases.<sup>19</sup> This is consistent with the finding for the Zr-H system studied here with computed  $\Delta E_{\text{ZPE}}^* + E_{\text{ZPE,H}_2}$  of  $-16.9 \text{ kJ mol}^{-1} \text{ H}_2$ . Thus, with  $\Delta S \approx 0.130 \text{ kJ K}^{-1} \text{ mol}^{-1} \text{ H}_2$ , the simplest calculation based only on DFT ground-state electronic energies can predict  $T_d$  to within approximately 150 K of the more rigorous computation that includes zero-point energies. This is supported by the results shown in Table III for all five metal hydrides studied.

For the five metal hydrides studied in this work, the lowest level of theory predicts  $T_d$  to within approximately 150 K of the more rigorous quasiharmonic predicted value with the largest differences apparent for the heavy metal hydrides. With the exception of HfH<sub>2</sub>, for which no experimental data could be found, the models including vibrational effects are within 70 K of the experimental values, and the simplest model predicts  $T_d$  to within 200 K of the experimental value. This suggests that material screening based on DFT calculations seeking to identify metal hydrides that are thermodynamically stable to the release of hydrogen at high temperatures could first screen a library of materials based on  $E_0$  alone. As previously discussed, the simple harmonic and ground-state

energies including zero-point vibration models require the same amount of computational effort with our method of computing vibrational energies.

For all materials tested, the quasiharmonic thermal expansion correction to the free energy was minor, and the zero-point energy correction to the ground-state volume shifted  $\Delta H$  at 0 K by less than 1.5 kJ mol<sup>-1</sup> H<sub>2</sub>. TiH<sub>2</sub>, ZrH<sub>2</sub>, HfH<sub>2</sub>, and NaH each had differences in the predicted  $T_d$  for the simple harmonic model at the uncorrected ground-state volume and the static quasiharmonic models of less than 30 K or 4 kJ mol<sup>-1</sup> H<sub>2</sub> with the approximation  $\Delta S = 0.130 \text{ kJ K}^{-1} \text{ mol}^{-1} \text{ H}_2$ . The largest difference between the quasiharmonic and simple harmonic calculations at the uncorrected ground-state volume was less than 70 K or 9 kJ mol<sup>-1</sup> H<sub>2</sub> for LiH. The quasiharmonic approximation estimates the volume dependence of the vibrational frequency and, consequently, the volume expansion of the solid phases. LiH melts at 961 K, and above this temperature, the appropriate phase system is a mixture of liquid LiH, liquid Li, and H<sub>2</sub> gas. The quasiharmonic approximation is not valid for temperatures approaching the melting point because anharmonic effects are no longer negligible.<sup>38</sup> In this two-liquid region, H<sub>2</sub> reaches a pressure of 1 atm ( $\approx 1 \text{ bar}$ ) at 1184 K.<sup>69,83</sup> This is only slightly larger than the simple harmonic and quasiharmonic predicted values of 1053 and 1118 K, respectively. Similarly, the predicted values of  $T_d$  for NaH are reasonably close to the experimental value considering that Na melts at low temperature. The performance of the thermodynamic models used in this work in predicting dissociation temperatures for metal-hydrogen systems with solids that melt at temperatures lower than  $T_d$  is due to the linear nature of  $\Delta G$ .

TABLE III.  $T_d$  (K) for metal hydrides predicted using both static quasiharmonic calculation of free energies and free energies based on ground-state energies at volumes uncorrected for zero-point-energy vibrational effects with and without zero-point energy. Published experimental values are included for comparison.  $\Delta S = 0.130 \text{ kJ K}^{-1} \text{ mol}^{-1} \text{ H}_2$ .

	Quasiharmonic $T_d = \frac{\Delta(E_0)}{\Delta S}$	$T_d = \frac{\Delta(E_0 + \text{ZPE})}{\Delta S}$		Experiment
LiH	1118	1124	1075	1184 (Ref. 69)
NaH	647	664	655	701 (Ref. 79)
TiH <sub>2</sub>	946	1088	941	916 (Refs. 80,81)
ZrH <sub>2</sub>	1129	1284	1154	1154 (Refs. 81,82)
HfH <sub>2</sub>	1003	1140	1001	

### E. Hydrogen isotope effects in metal hydrides

Isotope effects in metal hydrides arise due to differences in vibrational frequencies of hydrogen isotopes in a crystal lattice. Isotope effects are known to cause changes in equilibrium lattice constants and thermal conductivities, as well as shifts in phase-transition temperatures.<sup>43,84</sup> Zhernov and Inyushkin wrote a review article on changes in phonon modes due to isotope composition in crystals. They note that for a polyatomic crystal, the frequency shift of a vibrational mode is inversely proportional to  $M_c^{1/2}$ , the average mass of the crystal, and proportional to the square of the modulus of the associated polarization vector.<sup>43</sup> Thus, metal hydrides with heavier isotopes will have smaller vibrational contributions to the free energy.

Two papers investigating isotope effects in  $\text{TiX}_2$  and  $\text{LiX}$  using first-principles calculations have discussed the stability of isotope-substituted metal hydrides only in terms of the free energy of the metal hydride.<sup>38,44</sup> This led to the erroneous conclusion that metal hydrides substituted with heavier hydrogen isotopes are more stable over large temperature ranges. More correctly, however, the free energy of a metal hydride must be considered relative to that of other reaction products. For  $\text{TiX}_2$  and  $\text{LiX}$ , these include the pure metal species and, critically, the hydrogen gas isotope. We show in the following the relative stabilities of the isotope-substituted metal hydrides relative to the associated pure metal and hydrogen gas species are temperature dependent.

The thermodynamic stability of a metal hydride can be calculated with respect to formation of the pure metal phase and hydrogen gas. For  $\text{TiX}_2$ , where  $X = \text{H}, \text{D}, \text{or T}$ , the dehydrogenation reaction can be written as  $\text{TiX}_2 \leftrightarrow \text{Ti} + X_2$  and

$$\Delta G(T) = G_{\text{Ti}} + G_{X_2} - G_{\text{TiX}_2}. \quad (17)$$

Since

$$G = U + PV - TS = H - TS, \quad (18)$$

we can write

$$\Delta G = \Delta H + \Delta(-TS), \quad (19)$$

where the enthalpy of each solid species is the summation of the DFT electronic total energy and the vibrational contribution to the free energy determined from phonon calculations. The entropies of solid species are the vibrational entropies from phonon calculations, and the thermodynamic properties of the gaseous hydrogen isotope species are calculated as previously discussed. As written,  $\Delta H = -\Delta H_f$  for the metal hydride. As a reminder,  $\Delta G > 0$  indicates that the formation of the metal hydride is favored.

Figure 4 compares the magnitudes of the  $\Delta H$  and  $\Delta(-TS)$  terms for protium relative to deuterium and tritium in the  $\text{TiX}_2$  metal hydride system. These calculations were based on Eq. (10) with a cutoff energy of 350 eV and  $8 \times 8 \times 8$   $k$ -points for consistency with Hu *et al.*<sup>44</sup> Our calculations are similar to Hu *et al.* except for the use of PAW (GGA-PW91) rather than USPP (GGA-PW91). At low temperature, negative ( $\Delta G_H - \Delta G_D$ ) and ( $\Delta G_H - \Delta G_T$ ) indicate that the heavier isotopes are more thermodynamically stable to the pure metal and associated hydrogen gas species than  $\text{TiH}_2$ . The hydrogen

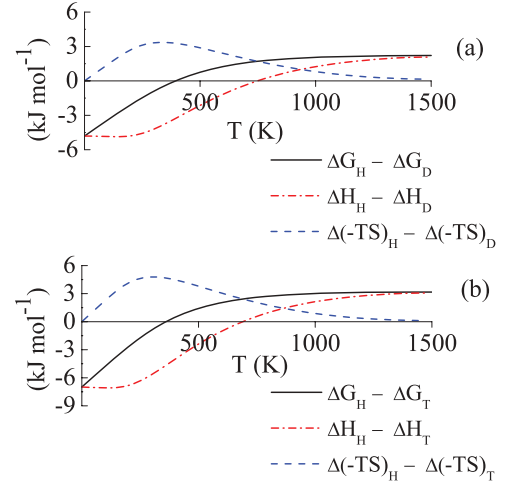


FIG. 4. (Color online) Temperature-dependent contributions of  $\Delta H$  and  $\Delta(-TS)$  to  $\Delta G = \Delta H + \Delta(-TS)$  for isotope-substituted  $\text{TiX}_2$  ( $X = \text{D}$  and  $\text{T}$ ) relative to  $\text{TiH}_2$  determined using a simple harmonic model of the free energy at the zero-point-energy corrected ground-state volume: (a)  $\text{TiD}_2$  relative to  $\text{TiH}_2$  and (b)  $\text{TiT}_2$  relative to  $\text{TiH}_2$ .

pressures in equilibrium with the solid species are ranked  $\text{TiT}_2 < \text{TiD}_2 < \text{TiH}_2$  at low temperature. Above 360 and 390 K for the tritide and deuteride, respectively, the relative stability ranking changes such that  $\text{TiH}_2 < \text{TiD}_2 < \text{TiT}_2$  in terms of hydrogen pressures. Wiswall and Reilly determined a similar crossover point experimentally at 445 K for  $\text{VH}_2$  and  $\text{VD}_2$ .<sup>84</sup> At 0 K,  $\Delta H_H - \Delta H_X$  is dominated by the difference in zero-point energies of the metal hydrides.

At high temperature, the difference in  $\Delta G$  between the isotope-substituted systems is again controlled by the enthalpy terms. The differences in the entropy terms reach constant values at high temperature. This trend was verified for  $\text{ZrX}_2$  and  $\text{LiX}$  up to 1500 K. It was found that the differences in entropy terms approach approximately constant negative values for protium relative to deuterium and tritium for both metal hydrides. Again, the enthalpy term dominates the difference in stability of the isotope-substituted species particularly for temperatures greater than 1000 K. However,  $\Delta H_H - \Delta H_X$  is dominated by the difference in vibrational internal energies of the gaseous species rather than the metal hydrides at the high temperatures studied. While at both low and high temperatures the differences in  $\Delta H$  dominate the stabilities of the hydrogen isotope-substituted metal hydrides

TABLE IV. Zero-point-energy correction to ground-state volume of metal hydrides due to hydrogen isotope mass  $(V_{0c} - V_0) V_0^{-1} \times 100\%$  where  $V_{0c}$  and  $V_0$  are the zero-point-energy corrected and uncorrected unit-cell volumes at 0 K.

X =	H	D	T
LiX	6.4	5.1	4.5
NaX	4.7	3.6	3.1
TiX <sub>2</sub>	3.2	2.3	1.9
ZrX <sub>2</sub>	2.5	1.8	1.5
HfX <sub>2</sub>	2.5	1.8	1.5



TABLE V.  $T_d$  (K) for metal hydrides predicted via simple harmonic calculation at the uncorrected ground-state volume.

$X =$	H	D	T	$\Delta T_d$ (H-D)	$\Delta T_d$ (H-T)
LiX	1053	1029	1020	24	33
NaX	620	591	579	29	41
TiX <sub>2</sub>	930	920	915	10	15
ZrX <sub>2</sub>	1108	1094	1089	14	19
HfX <sub>2</sub>	986	974	969	12	17

relative to the pure metal and associated gas species, at intermediate temperatures, the stability is a balance between entropic and enthalpic terms.

The quasiharmonic approximation corrects equilibrium volumes for lattice vibrations. The magnitude of the correction to the unit-cell volume for various metal hydrides at 0 K due to isotopic mass is shown in Table IV. The volume changes are presented as percentages of the uncorrected volume. The magnitude of the zero-point-energy correction for a given metal hydride depends on the slope of the vibrational free-energy curve  $F^{\text{qh}}(V, 0 \text{ K})$  and the shape of  $E_0(V)$ . The correction magnitude decreases for heavier isotopes and similarly decreases for heavier metal atoms.

For the NGNP application described in the Introduction, metal hydrides can be considered as potential tritium sequestration materials at elevated temperatures. We have already shown for TiX<sub>2</sub> that heavier hydrogen isotopes destabilize metal hydrides above a critical temperature, but how much does this shift  $T_d$  at 1 bar hydrogen pressure? Table V presents the predicted stabilities in terms of  $T_d$  for each of the hydrogen isotope-substituted metal hydrides studied based on a simple harmonic calculation at  $V_0$ . The results of the simple harmonic calculation are very similar to those of the more computationally intensive quasiharmonic approximation with the largest differences for the lightest metals, and the order of the stabilities is unchanged using the lower level of theory. As expected, metal hydrides substituted with lighter hydrogen isotopes are more thermodynamically stable beyond low temperatures. However, since  $T_d$  of the protide is within 50 K of the deuteride and tritide for each of the materials studied, calculations simply based on protium are expected to yield an adequate description of the thermodynamic stability of metal hydrides for operation with tritium. This is useful because protiated metal hydrides have

largely been the focus of both experimental and theoretical studies.

## V. CONCLUSIONS

We have presented an investigation into the predicted thermodynamic stabilities of five metal hydrides using four different levels of theory. These levels of theory included predictions based solely on ground-state energies, simple harmonic calculations at a single volume, quasiharmonic calculations, and inclusion of an explicit anharmonic correction to the quasiharmonic free energy. The two highest levels of theory include estimates of thermal expansion. Our aim was to determine the minimum amount of computational effort required to reliably predict  $\Delta G(T)$  and  $T_d$  for metal hydrides and also to determine if inclusion of hydrogen isotopes affects the predicted stability by a significant amount. Our calculations show that the levels of theory that account for volume expansion produce only a minor correction to the free energies of the metals and metal hydrides within the temperature range of interest. The simplest model based on DFT ground-state electronic energies without zero-point-energy correction was shown to predict  $T_d$  within 200 K of the experimental values. Higher-order models including vibrational free energies predicted  $T_d$  to within 70 K of the available experimental values. Since the simple harmonic calculation predicted stabilities within 70 K of the quasiharmonic values with largest differences for the lightest materials, an efficient screening method to identify very stable metal hydrides would first screen based on  $\Delta E_0$  and then investigate interesting materials more thoroughly with a simple harmonic calculation at the uncorrected ground-state volume.

We have also confirmed the previously known observation that the relative stabilities of metal hydrides substituted with hydrogen isotopes are temperature dependent. At low temperatures, metal hydrides substituted with heavier hydrogen isotopes are more thermodynamically stable to decomposition, but this ranking changes at high temperature. In all cases,  $T_d$  for the protiated metal hydrides are within 50 K of the deuterides and tritides. Thus, for material screening purposes, hydrogen isotope effects can be neglected.

## ACKNOWLEDGMENT

This research was performed using funding received from the DOE Office of Nuclear Energy's Nuclear Energy University Programs.

<sup>1</sup>U.S. DOE Office of Nuclear Energy, Next Generation Nuclear Plant Report to Congress, April 2010.

<sup>2</sup>U.S. DOE Nuclear Energy Research Advisory Committee and Generation IV International Forum, A Technology Roadmap for Generation IV Nuclear Energy Systems (03-GA50034) Dec. 2002.

<sup>3</sup>H. Smithson, C. A. Marianetti, D. Morgan, A. Van der Ven, A. Predith, and G. Ceder, *Phys. Rev. B* **66**, 144107 (2002).

<sup>4</sup>K. Miwa and A. Fukumoto, *Phys. Rev. B* **65**, 155114 (2002).

<sup>5</sup>Y. Song, Z. X. Guo, and R. Yang, *Phys. Rev. B* **69**, 094205 (2004).

<sup>6</sup>Y. Song, W. C. Zhang, and R. Yang, *Int. J. Hydrogen Energy* **34**, 1389 (2009).

<sup>7</sup>T. J. Frankcombe and G.-J. Kroes, *Phys. Rev. B* **73**, 174302 (2006).

<sup>8</sup>C. Wolverton, V. Ozoliņš, and M. Asta, *Phys. Rev. B* **69**, 144109 (2004).

<sup>9</sup>X. Z. Ke, A. Kuwabara, and I. Tanaka, *Phys. Rev. B* **71**, 184107 (2005).

<sup>10</sup>G. J. Ackland, *Phys. Rev. Lett.* **80**, 2233 (1998).

- <sup>11</sup>C. Wolverton and V. Ozoliņš, *Phys. Rev. B* **75**, 064101 (2007).
- <sup>12</sup>C. Wolverton, D. J. Siegel, A. R. Akbarzadeh, and V. Ozoliņš, *J. Phys.: Condens. Matter* **20**, 064228 (2008).
- <sup>13</sup>V. Ozoliņš, E. H. Majzoub, and C. Wolverton, *Phys. Rev. Lett.* **100**, 135501 (2008).
- <sup>14</sup>E. H. Majzoub and V. Ozoliņš, *Phys. Rev. B* **77**, 104115 (2008).
- <sup>15</sup>Y. Nakamori, K. Miwa, A. Ninomiya, H. Li, N. Ohba, S. I. Towata, A. Züttel, and S. I. Orimo, *Phys. Rev. B* **74**, 045126 (2006).
- <sup>16</sup>J. S. Hummelshøj *et al.*, *J. Chem. Phys.* **131**, 014101 (2009).
- <sup>17</sup>V. Ozoliņš, A. R. Akbarzadeh, H. Gunaydin, K. Michel, C. Wolverton, and E. H. Majzoub, *J. Phys. Conf. Ser.* **180**, 012076 (2009).
- <sup>18</sup>D. J. Siegel, C. Wolverton, and V. Ozoliņš, *Phys. Rev. B* **76**, 134102 (2007).
- <sup>19</sup>S. V. Alapati, J. K. Johnson, and D. S. Sholl, *Phys. Chem. Chem. Phys.* **9**, 1438 (2007).
- <sup>20</sup>S. V. Alapati, J. K. Johnson, and D. S. Sholl, *J. Phys. Chem. B* **110**, 8769 (2006).
- <sup>21</sup>S. V. Alapati, J. K. Johnson, and D. S. Sholl, *J. Phys. Chem. C* **111**, 1584 (2007).
- <sup>22</sup>S. V. Alapati, J. K. Johnson, and D. S. Sholl, *J. Alloys Compd.* **446-447**, 23 (2007).
- <sup>23</sup>S. V. Alapati, J. K. Johnson, and D. S. Sholl, *J. Phys. Chem. C* **112**, 5258 (2008).
- <sup>24</sup>S. M. Opalka, O. M. Lovvik, S. C. Emerson, Y. She, and T. H. Vanderspurt, *J. Membr. Sci.* **375**, 96 (2011).
- <sup>25</sup>H. R. Gong, *Intermetallics* **17**, 562 (2009).
- <sup>26</sup>N. Ozawa, N. B. Arboleda, Jr., H. Nakanishi, and H. Kasai, *Surf. Sci.* **602**, 859 (2008).
- <sup>27</sup>C. Y. Ouyang and Y. S. Lee, *Phys. Rev. B* **83**, 045111 (2011).
- <sup>28</sup>O. Y. Vekilova, D. I. Bazhanov, S. I. Simak, and I. A. Abrikosov, *Phys. Rev. B* **80**, 024101 (2009).
- <sup>29</sup>S. Hao and D. S. Sholl, *J. Membr. Sci.* **381**, 192 (2011).
- <sup>30</sup>S. Kang, S. Hao, and D. S. Sholl, in *Membrane Science and Technology*, edited by S. T. Oyama and S. M. Stagg-Williams (Elsevier, Amsterdam, 2011), Vol. 14, p. 309.
- <sup>31</sup>C. Ling, L. Semidey-Flecha, and D. S. Sholl, *J. Membr. Sci.* **371**, 189 (2011).
- <sup>32</sup>S. Hao and D. S. Sholl, *J. Membr. Sci.* **350**, 402 (2010).
- <sup>33</sup>S. Hao and D. S. Sholl, *Energy Environ. Sci.* **1**, 175 (2008).
- <sup>34</sup>C. G. Sonwane, J. Wilcox, and Y. H. Ma, *J. Phys. Chem. B* **110**, 24549 (2006).
- <sup>35</sup>K. Konashi, B. A. Pudjanto, T. Terai, and M. Yamawaki, *J. Phys. Chem. Solids* **66**, 625 (2005).
- <sup>36</sup>W. Bartscher, J. Rebizant, and J. M. Haschke, *J. Less-Common Met.* **136**, 385 (1988).
- <sup>37</sup>W. Zhu, R. Wang, G. Shu, P. Wu, and H. Xiao, *J. Phys. Chem. C* **114**, 22361 (2010).
- <sup>38</sup>H. F. Zhang, Y. Yu, Y. N. Zhao, W. H. Xue, and T. Gao, *J. Phys. Chem. Solids* **71**, 976 (2010).
- <sup>39</sup>M. T. Simnad, *Nucl. Eng. Des.* **64**, 403 (1981).
- <sup>40</sup>B. Sakintuna, F. Lamari-Darkrim, and M. Hirscher, *Int. J. Hydrogen Energy* **32**, 1121 (2007).
- <sup>41</sup>L. George and S. K. Saxena, *Int. J. Hydrogen Energy* **35**, 5454 (2010).
- <sup>42</sup>H. L. Yakel, Jr., *Acta Crystallogr.* **11**, 46 (1958).
- <sup>43</sup>A. P. Zhernov and A. V. Inyushkin, *Phys. Usp.* **44**, 785 (2001).
- <sup>44</sup>C. H. Hu, D. M. Chen, Y. M. Wang, and K. Yang, *J. Alloys Compd.* **450**, 369 (2008).
- <sup>45</sup>W. Grochala and P. P. Edwards, *Chem. Rev.* **104**, 1283 (2004).
- <sup>46</sup>J. J. Vajo, F. Mertens, C. C. Ahn, R. C. Bowman, Jr., and B. Fultz, *J. Phys. Chem. B* **108**, 13977 (2004).
- <sup>47</sup>G. J. Ackland, *J. Phys.: Condens. Matter* **14**, 2975 (2002).
- <sup>48</sup>B. Grabowski, T. Hickel, and J. Neugebauer, *Phys. Rev. B* **76**, 024309 (2007).
- <sup>49</sup>B. Grabowski, P. Söderlind, T. Hickel, and J. Neugebauer, *Phys. Rev. B* **84**, 214107 (2011).
- <sup>50</sup>K. Parlinski, software PHONON, 2005.
- <sup>51</sup>Z. Wu, *Phys. Rev. B* **81**, 172301 (2010).
- <sup>52</sup>Z. Wu and R. M. Wentzcovitch, *Phys. Rev. B* **79**, 104304 (2009).
- <sup>53</sup>A. Züttel, P. Wenger, S. Rentsch, P. Sudan, P. Mauron, and C. Emmenegger, *J. Power Sources* **118**, 1 (2003).
- <sup>54</sup>Y. Nie and Y. Xie, *Phys. Rev. B* **75**, 174117 (2007).
- <sup>55</sup>P. Carrier, R. Wentzcovitch, and J. Tsuchiya, *Phys. Rev. B* **76**, 064116 (2007).
- <sup>56</sup>B. Grabowski, L. Ismer, T. Hickel, and J. Neugebauer, *Phys. Rev. B* **79**, 134106 (2009).
- <sup>57</sup>L. Vočadlo and D. Alfè, *Phys. Rev. B* **65**, 214105 (2002).
- <sup>58</sup>T. Hickel, B. Grabowski, F. Körmann, and J. Neugebauer, *J. Phys.: Condens. Matter* **24**, 053202 (2012).
- <sup>59</sup>G. Kresse and J. Hafner, *Phys. Rev. B* **47**, 558 (1993).
- <sup>60</sup>G. Kresse and J. Hafner, *Phys. Rev. B* **49**, 14251 (1994).
- <sup>61</sup>G. Kresse and J. Furthmüller, *Phys. Rev. B* **54**, 11169 (1996).
- <sup>62</sup>G. Kresse and J. Furthmüller, *Comput. Mater. Sci.* **6**, 15 (1996).
- <sup>63</sup>D. S. Sholl and J. A. Steckel, *Density Functional Theory: A Practical Introduction* (Wiley, Hoboken, NJ, 2009).
- <sup>64</sup>P. E. Blöchl, *Phys. Rev. B* **50**, 17953 (1994).
- <sup>65</sup>G. Kresse and D. Joubert, *Phys. Rev. B* **59**, 1758 (1999).
- <sup>66</sup>J. P. Perdew, J. A. Chevary, S. H. Vosko, K. A. Jackson, M. R. Pederson, D. J. Singh, and C. Fiolhais, *Phys. Rev. B* **46**, 6671 (1992).
- <sup>67</sup>G. Bergerhoff and I. D. Brown, in *Crystallographic Databases*, edited by F. H. Allen, G. Bergerhoff and R. Severs (International Union of Crystallography, Chester, 1987).
- <sup>68</sup>FIZ Karlsruhe and NIST, The Inorganic Crystal Structure Database (ICSD).
- <sup>69</sup>J. Sangster and A. D. Pélon, *J. Phase Equilib.* **14**, 373 (1993).
- <sup>70</sup>F. E. Pretzel, G. N. Rupert, C. L. Mader, E. K. Storms, G. V. Gritton, and C. C. Rushing, *J. Phys. Chem. Solids* **16**, 10 (1960).
- <sup>71</sup>*NIST Chemistry Webbook, NIST Standard Reference Database Number 69*, edited by P. J. Linstrom and W. G. Mallard (National Institute of Standards and Technology, Gaithersburg, MD, 2011).
- <sup>72</sup>Thermodynamics Research Center, *TRC Thermodynamic Tables-Non-Hydrocarbons* (Texas A&M University System, College Station, TX. National Institute of Standards and Technology, Boulder, CO, extant 2001), r-20,21 (1986); s-20,21 (1986).
- <sup>73</sup>M. W. Chase Jr. ed., *NIST JANAF Thermochemical Tables* (J. Phys. Chem. Ref. Data Monograph No. 9, 1998).
- <sup>74</sup>G. B. Skinner and H. L. Johnston, *J. Chem. Phys.* **21**, 1383 (1953).
- <sup>75</sup>E. S. Fisher and C. J. Renken, *Phys. Rev.* **135**, A482 (1964).
- <sup>76</sup>E. Zuzek, J. P. Abriata, A. San-Martin, and F. D. Manchester, *J. Phase Equilib.* **11**, 385 (1990).
- <sup>77</sup>C. P. Kempter, R. O. Elliott, and K. A. Gschneidner, *J. Chem. Phys.* **33**, 837 (1960).
- <sup>78</sup>*American Institute of Physics Handbook*, edited by D. E. Gray (McGraw Hill, New York, 1972).

<sup>79</sup>C. Qui, S. M. Opalka, G. B. Olson, and D. L. Anton, *Int. J. Mater. Res.* **97**, 845 (2006).

<sup>80</sup>W. M. Mueller, *Metal Hydrides* (Academic, New York, 1968), p. 336.

<sup>81</sup>G. Sandroock and G. Thomas, *Appl. Phys. A* **72**, 153 (2001).

<sup>82</sup>R. L. Beck and W. M. Mueller, *Metal Hydrides* (Academic, New York, 1968), p. 241.

<sup>83</sup>E. Veleckis, *J. Nucl. Mater.* **79**, 20 (1979).

<sup>84</sup>R. H. Wiswall, Jr. and J. J. Reilly, *Inorg. Chem.* **11**, 1691 (1972).